

Two-dimensional bright and dark-in-bright dipolar Bose-Einstein condensate solitons on a one-dimensional optical lattice

S. K. Adhikari [‡]

Instituto de Física Teórica, UNESP - Universidade Estadual Paulista, 01.140-070 São Paulo, São Paulo, Brazil

Abstract.

We study the statics and dynamics of anisotropic, stable, bright and dark-in-bright dipolar quasi-two-dimensional Bose-Einstein condensate (BEC) solitons on a one-dimensional (1D) optical-lattice (OL) potential. These solitons mobile in a plane perpendicular to the 1D OL trap can have both repulsive and attractive contact interactions. The dark-in-bright solitons are the excited states of the bright solitons. The solitons, when subject to a small perturbation, exhibit sustained breathing oscillation. The dark-in-bright solitons can be created by phase imprinting a bright soliton. At medium velocities the collision between two solitons is found to be quasi elastic. The results are demonstrated by a numerical simulation of the three-dimensional mean-field Gross-Pitaevskii equation in three spatial dimensions employing realistic interaction parameters for a dipolar ^{164}Dy BEC.

PACS numbers: 03.75.Lm, 03.75.Kk, 03.75.Hh

[‡] adhikari@ift.unesp.br; URL: <http://www.ift.unesp.br/users/adhikari>

1. Introduction

A bright soliton can travel with a constant velocity in one dimension (1D) maintaining its shape due to a cancellation of nonlinear attraction and dispersive repulsion. Solitons have been studied in water wave, Bose-Einstein condensates (BEC) [1] and nonlinear optics [2]. Of these, solitons in BEC have drawn much attention lately because of its inherent quantum interaction. Quasi-1D bright matter-wave solitons were predicted [3] for *attractive* atomic interaction and created in BECs of ^7Li [4, 5] and ^{85}Rb [6] atoms by adjusting the atomic contact interaction to a suitable attractive value using a Feshbach resonance [7]. Due to collapse instability for attractive contact interaction in alkali-metal-atom BECs, (a) one cannot have a quasi-two-dimensional (quasi-2D) bright soliton for a cubic nonlinearity, and (b) the usual quasi-1D bright solitons can accommodate a small number of atoms [4, 6].

The recent observation of dipolar BECs of ^{52}Cr [8], ^{164}Dy [9] and ^{168}Er [10] atoms have started a great deal of activity in this area [11, 12, 13, 14, 15, 16, 17, 18, 19, 20] including new investigation of BEC solitons in a different scenario. Apart from quasi-1D bright dipolar BEC solitons [21], asymmetric quasi-2D bright [22, 23, 24, 25, 26, 27, 28] and vortex [29, 30] solitons have been predicted. Also, in a dipolar BEC, unlike in a nondipolar BEC, these solitons can be realized for a repulsive contact interaction. Consequently, one can have a robust dipolar soliton which can accommodate a large number of atoms. There have been studies of collision of quasi-1D [21, 31] and quasi-2D [26, 29, 23] dipolar solitons.

In this paper we study the statics and dynamics of quasi-2D dipolar bright and dark-in-bright solitons mobile in the $x - z$ plane and trapped along the y axis by a 1D periodic optical lattice (OL) potential. The dipolar atoms will always be considered polarized along the z direction. A periodic OL potential cannot localize a BEC to form a bright soliton with only repulsive contact interaction, although, localized gap solitons in the band-gap of a periodic OL potential can be formed in a repulsive nondipolar [32] and dipolar [33] BEC. The gap solitons are trapped in all directions and hence cannot move freely like a bright soliton without trap in certain direction(s). Because of the anisotropic nature of the dipolar interaction and the OL potential, the bright and dark-in-bright quasi-2D dipolar solitons, which we consider here, have a fully anisotropic shape. For a small strength of the OL potential, the quasi-2D soliton extends over several OL sites in the y direction. However, for a moderate strength of the OL potential and for a moderate number of dipolar atoms, compact quasi-2D solitons occupying a single OL site can be formed and we will be mostly interested in such compact solitons. For a large number of dipolar atoms with dominating dipolar interaction the quasi-2D solitons collapse due to an excess of dipolar energy as in a trapped dipolar BEC [34] and when the contact atomic repulsion dominates over the dipolar interaction the atoms escape to infinity and no soliton can be formed. The result of the present study is illustrated using the numerical solution of the time-dependent three-dimensional (3D) mean-field Gross-Pitaevskii (GP) equation [47] using realistic values of the interaction parameters

of ^{164}Dy atoms [9].

These quasi-2D dark-in-bright solitons are themselves bright solitons mobile in the $x - z$ plane and are excited states of the quasi-2D bright solitons with a notch (zero in density), for example, along $x = 0$ or $z = 0$. The dark-in-bright solitons with a zero in the middle are similar to the lowest odd-parity excited states of the harmonic oscillator potential. Dark solitons in a confined BEC have been observed experimentally [35, 37, 36]. The dark solitons with a notch imprinted [35, 38] on a trapped repulsive BEC are dynamically unstable and are destroyed by snake instability [41, 42, 43, 44, 45, 46, 39, 40]. Such instability can be reduced as the confining trap is made weaker [39]. The present dark-in-bright solitons created on quasi-2D solitons are not subject to any confining trap in the $x - z$ plane and do not exhibit any kind of dynamical instability.

To study the stability of the quasi-2D solitons we performed two tests. The solitons are found to exhibit sustained breathing oscillation upon a small perturbation, introduced by a change in the scattering length, confirming their stability. Such a change in scattering length can be realized experimentally by varying a uniform background magnetic field near a Feshbach resonance [7]. As a more stringent test, we demonstrate the generation of a dark-in-bright soliton by introducing an extra phase of π on one half of the wave function (phase imprinting). Such a phase can be introduced in a laboratory using the dipole potential of a far detuned laser beam [35, 38]. In a numerical real-time simulation of the mean-field model such a phase-imprinted profile is used as the initial state, which quickly transforms into a quasi-2D dark-in-bright soliton without exhibiting any dynamical instability at large times.

At medium velocities the frontal collision between two quasi-2D solitons is found to be quasi elastic while the two solitons come out without any visible deformation in shape. Only in 1D the collision between two analytic solitons is truly elastic. However, inelastic nature of the collision is expected at very low velocities in the case of two quasi-2D dipolar solitons.

2. Mean-field model

At ultra-low temperatures the properties of a dipolar condensate of N atoms, each of mass m , can be described by the mean-field GP equation, for the wave function $\phi(\mathbf{r}, t)$, with nonlocal nonlinearity of the form: [50, 49]

$$i\hbar \frac{\partial \phi(\mathbf{r}, t)}{\partial t} = \left[-\frac{\hbar^2}{2m} \nabla^2 + V_{\text{trap}}(\mathbf{r}) + \frac{4\pi\hbar^2 a N}{m} |\phi(\mathbf{r}, t)|^2 + N \int U_{\text{dd}}(\mathbf{r} - \mathbf{r}') |\phi(\mathbf{r}', t)|^2 d\mathbf{r}' \right] \phi(\mathbf{r}, t), \quad (1)$$

where $\int d\mathbf{r} |\phi(\mathbf{r}, t)|^2 = 1$ and a is the scattering length. To study the 2D solitons mobile in the $x - z$ plane we consider the following harmonic (H) or OL potential in the y direction

$$V_{\text{trap}}^{\text{H}}(\mathbf{r}) = \frac{1}{2} m \omega^2 y^2, \quad (2)$$

$$V_{\text{trap}}^{\text{OL}}(\mathbf{r}) = sE_R \sin^2\left(\frac{2\pi}{\lambda}y\right), \quad (3)$$

respectively, where ω is the frequency of the harmonic trap, s is the strength of the OL trap in units of recoil energy $E_R = \hbar^2/(2m\lambda^2)$ where λ is the wave length of the lattice. The dipolar interaction, for magnetic dipoles, is [50]

$$U_{\text{dd}}(\mathbf{R}) \equiv \frac{\mu_0\mu^2}{4\pi}\mathbf{V}_{\text{dd}}(\mathbf{R}) = \frac{\mu_0\mu^2}{4\pi}\frac{\mathbf{1} - 3\cos^2\theta}{|\mathbf{R}|^3}, \quad (4)$$

where $\mathbf{R} = \mathbf{r} - \mathbf{r}'$ determines the relative position of dipoles and θ is the angle between \mathbf{R} and the direction of polarization z , μ_0 is the permeability of free space and μ is the dipole moment of an atom. The strength of dipolar interaction can be expressed in terms of a dipolar length a_{dd} defined by [50]

$$a_{\text{dd}} \equiv \frac{\mu_0\mu^2m}{12\pi\hbar^2}. \quad (5)$$

For the formation of a quasi-2D soliton, mobile in the $x - z$ plane, a dimensionless GP equation for the dipolar BEC soliton can be written as [50, 21]

$$\begin{aligned} i\frac{\partial\phi(\mathbf{r},t)}{\partial t} = & \left[-\frac{\nabla^2}{2} + V(y) + g|\phi(\mathbf{r},t)|^2 \right. \\ & \left. + g_{\text{dd}} \int V_{\text{dd}}(\mathbf{R})|\phi(\mathbf{r}',t)|^2 d\mathbf{r}' \right] \phi(\mathbf{r},t), \end{aligned} \quad (6)$$

with

$$V^{\text{H}}(y) = \frac{1}{2}y^2, \quad V^{\text{OL}}(y) = \frac{s}{2}\sin^2 y, \quad (7)$$

for the harmonic trap (2) and the OL trap (3), respectively, where $g = 4\pi aN$, $g_{\text{dd}} = 3Na_{\text{dd}}$. In the case of the harmonic trap, length is expressed in (6) in units of oscillator length $l = \sqrt{\hbar/(m\omega)}$, energy in units of oscillator energy $\hbar\omega$, probability density $|\phi|^2$ in units of l^{-3} , and time in units of $t_0 = 1/\omega$. In the case of the OL trap, length is expressed in units of $l = \lambda/(2\pi)$, energy in units of recoil energy E_R , probability density $|\phi|^2$ in units of l^{-3} , and time in units of $t_0 = m\lambda^2/(2\pi\hbar)$.

3. Numerical Results

We consider ^{164}Dy atoms in this study of BEC solitons. The magnetic moment of a ^{164}Dy atom is $\mu = 10\mu_B$ [9] with μ_B the Bohr magneton leading to the dipolar lengths $a_{\text{dd}}(^{164}\text{Dy}) \approx 132.7a_0$, with a_0 the Bohr radius. The dipolar interaction in ^{164}Dy atoms is roughly eight times larger than that in ^{52}Cr atoms with a dipolar length $a_{\text{dd}}(^{52}\text{Cr}) \approx 15.3a_0$ [50]. Because of the large magnetic moment, the dipolar ^{164}Dy BEC will facilitate the formation of bright and dark-in-bright solitons.

The time-dependent GP equation (6) can be solved by different numerical methods [48, 51]. We solve the GP equation by the split-step Crank-Nicolson method [48, 52] with real- and imaginary-time propagation in Cartesian spatial coordinates using a space step of 0.1 and a time step of 0.0002 for a soliton of smaller size and a space step of 0.2 and a time step of 0.001 for a soliton of larger size. We employ the computer programs of

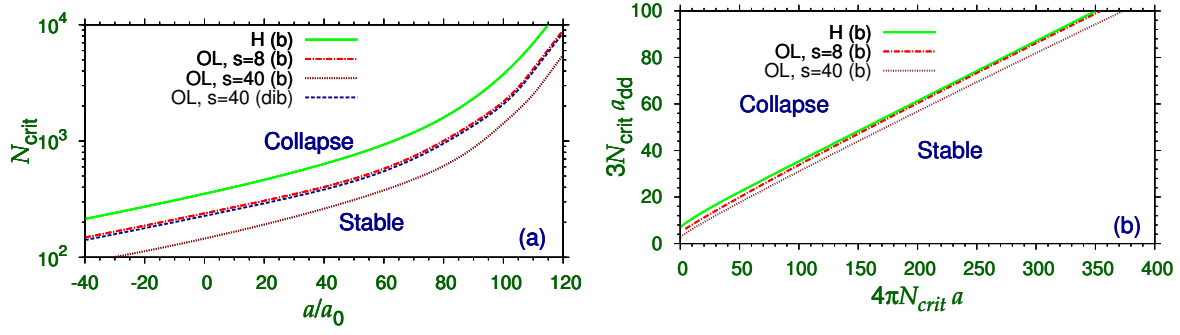


Figure 1. (Color online) (a) A $N_{\text{crit}} - a$ phase plot illustrating the parameter space for the formation of a stable quasi-2D bright (b) and dark-in-bright (dib) soliton in a ^{164}Dy BEC with $a_{\text{dd}} = 132.7a_0$ for harmonic (H) and OL traps. The soliton is stable for $N < N_{\text{crit}}$ and collapses for $N > N_{\text{crit}}$. (b) A universal $g_{\text{dd}} - g$ phase plot showing the stability region of a quasi-2D bright soliton applicable to a BEC of any dipolar atom. All quantities plotted in this and other figures are dimensionless. In all calculations of this paper the length scale $l = 1 \mu\text{m}$.

Refs. [47, 53, 54, 52] for this purpose. As the bright and dark-in-bright solitons are the ground states with specific parity, they can be obtained by imaginary-time propagation. The stability of the solitons is studied by real-time propagation.

To obtain a bright soliton in numerical simulation we consider the following initial Gaussian wave function

$$\phi(\mathbf{r}) = \frac{\pi^{-3/4}}{\sqrt{w_x w_y w_z}} \exp \left[-\frac{x^2}{2w_x^2} - \frac{y^2}{2w_y^2} - \frac{z^2}{2w_z^2} \right], \quad (8)$$

where w_x, w_y and w_z are the widths along x, y and z axes, respectively. For a dark-in-bright soliton, for example, with a notch along $x = 0$, we consider the initial function

$$\phi(\mathbf{r}) = \frac{\sqrt{2}x}{\sqrt{\pi^{3/2} w_x^3 w_y w_z}} \exp \left[-\frac{x^2}{2w_x^2} - \frac{y^2}{2w_y^2} - \frac{z^2}{2w_z^2} \right]. \quad (9)$$

A quasi-2D bright soliton was obtained by solving the 3D GP equation (6) by imaginary-time propagation using the initial function (8) with conveniently chosen widths for different values of number of atoms N and scattering length a . For a dominating dipolar interaction ($a_{\text{dd}} > a$), the bright solitons are possible for a moderate number of atoms. The system collapses as the number of atoms is increased beyond a critical number N_{crit} due to an excess of dipolar energy density [34]. For a dominating contact repulsion ($a_{\text{dd}} < a$), no solitons can be formed. The stability region for the formation of a quasi-2D soliton in the parameter space for ^{164}Dy atoms is obtained from a imaginary-time propagation of (6) in the same way as in Refs. [55, 56] for a nondipolar trapped BEC. For a small number of atoms ($N \sim 100$) and scattering length a ($< a_{\text{dd}}$) a quasi-2D bright soliton is numerically obtained by imaginary-time propagation starting from the initial Gaussian profile (8). Then the calculation is repeated increasing the number of atoms N keeping all other parameters fixed. No such soliton can be obtained numerically for N greater than the critical number N_{crit} . The result of our finding is

illustrated in the $N_{\text{crit}} - a$ phase plot of figure 1(a) showing the critical number N_{crit} for a harmonic trap as well as an OL trap with two strengths: $s = 8$ and 40. We also plot in this figure the critical number of the dark-in-bright soliton on the OL potential of strength $s = 40$ obtained by imaginary-time simulation starting from the initial function (9) in a similar fashion. Although, the case of the harmonic potential has been studied before and in the following we present only results for the OL potential, we include the results of the harmonic potential in the phase plot of figure 1 to address the difference between the two cases. The critical number of atoms increases with the increase of scattering length a . The bright solitons are unconditionally stable and last for ever in real-time propagation without any visible change of shape. Although, the stability plot of figure 1(a) is closely related to the parameters of ^{164}Dy atoms, a more universal $g - g_{\text{dd}}$ plot as shown in figure 1(b) is applicable to any dipolar BEC. The universal stability line of figure 1(b) has the approximate straight line shape and can be easily extrapolated to the case of larger nonlinearities g and g_{dd} .

The 1D harmonic and OL potentials along y direction are quite different and it is of interest to know how this changes the stability and shape of the quasi-2D solitons. We will mostly study the quasi-2D OL solitons in a deep OL trap when the quasi-2D soliton occupies a single OL site. The harmonic trap is wide and can accommodate a larger number of atoms in a larger spatial extension compared to the OL trap which can accommodate a smaller number of atoms in a single site with a smaller spatial extension. For a large number of atoms in the same OL trap the dipolar energy density will be too large to provoke collapse instability [34], viz. figure 1. However, as the strength s of the OL is lowered from 40 to 8, some atoms can tunnel to the adjacent site. This reduces the central dipolar energy density and collapse instability, thus accommodating a larger number of atoms in a shallow OL potential as can be seen in figure 1. The dark-in-bright soliton is an excited state of the bright soliton with a zero in the middle and has a much larger spatial extension with a smaller dipolar energy density and hence can accommodate a larger number of atoms as can be seen by comparing the plots marked “b” and “dib” for $s = 40$ in figure 1(a). The shape (aspect ratio in the 2D plane and not the actual size) of the quasi-2D solitons in the case of a harmonic and deep OL potential is determined completely by the dipolar interaction and not the confining trap. However, the actual size of these solitons will be determined by both the confining potential and dipolar interaction. Hence these quasi-2D solitons have a similar shape (not size) in the 2D plane, independent of the trapping potential. For a shallow OL potential quasi-2D solitons occupying a few OL sites can be formed close to the stability line in figure 1. To the right and away from the stability line, the atomic contact repulsion increases and the soliton may extend to several OL sites and eventually will be delocalized for an excess of contact repulsion. The quasi-2D solitons on a harmonic potential has been thoroughly studied before [22, 23, 24, 25, 26] and we present a comprehensive study of the quasi-2D solitons on an OL potential in the following.

In figures 2 (a) – (f) we display the 3D isodensity profile of the quasi-2D bright solitons for different N, a and s , obtained by imaginary-time propagation of the GP

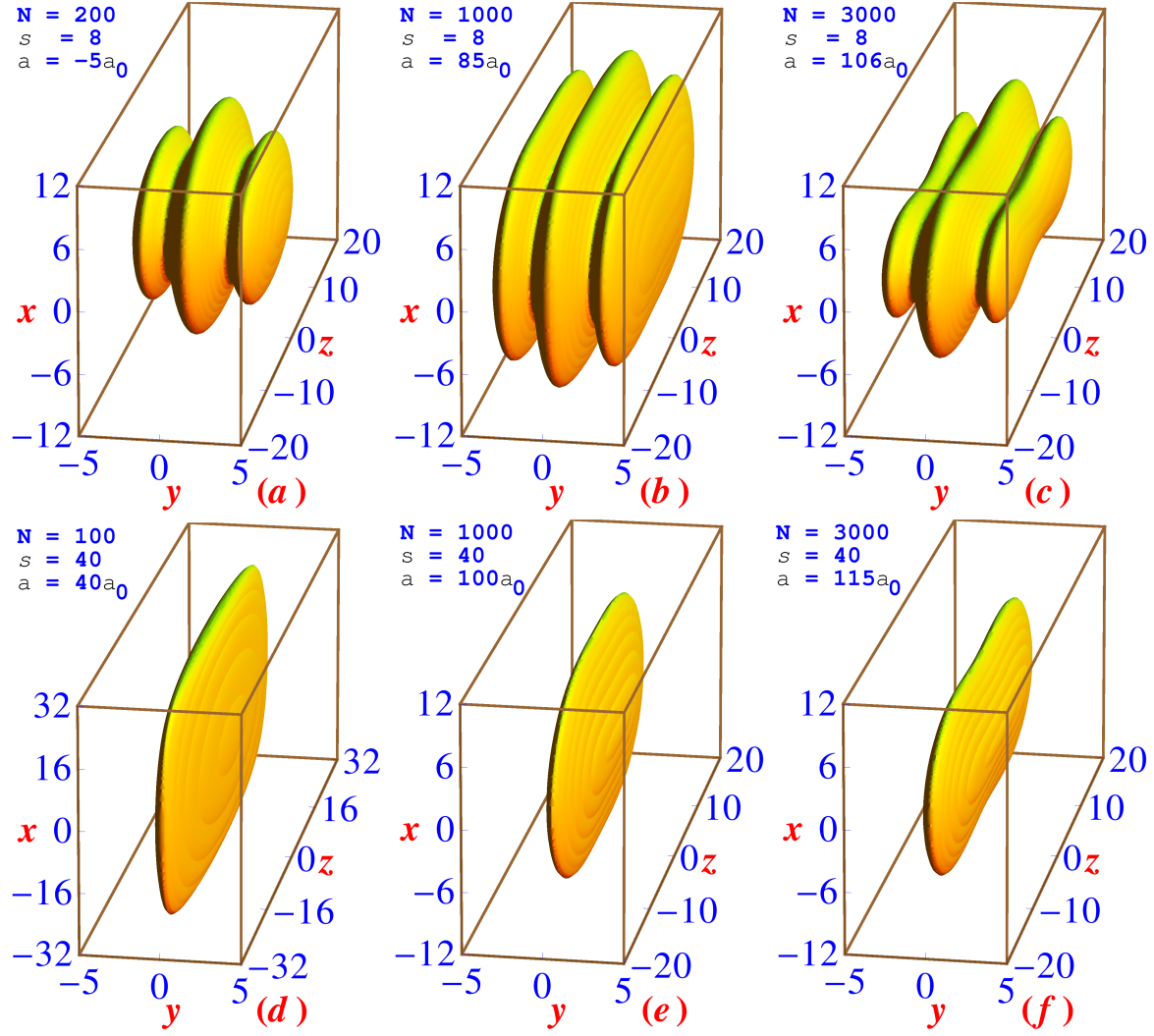


Figure 2. (Color online) 3D isodensity contour $|\phi(\mathbf{r})|^2$ of a bright soliton of ^{164}Dy atoms in the OL trap $V(y) = s \sin^2 y/2$ for (a) $a = -5a_0, N = 200, s = 8$, (b) $a = 85a_0, N = 1000, s = 8$, (c) $a = 106a_0, N = 3000, s = 8$, (d) $a = 40a_0, N = 100, s = 40$, (e) $a = 100a_0, N = 1000, s = 40$, and (f) $a = 115a_0, N = 3000, s = 40$. The dimensionless density on the contour is 0.000001. With present length scale $l = 1 \mu\text{m}$ this density corresponds to 10^6 atoms/ cm^3 . The central density of the solitons is typically 10^{10} atoms/ cm^3 .

equation with the OL potential starting with the initial wave function (8). Because of the OL trap in the y direction, the solitons have a quasi-2D shape in the $x - z$ plane, as can be seen in figure 2. In this figure we present results for two strengths of the OL potential: $s = 8$ and 40. Of these, $s = 8$ corresponds to a weaker OL trap and the quasi-2D solitons extend over several sites of the OL potential. Compact quasi-2D solitons occupying a single site of the OL trap is possible for $s = 40$. The size of the soliton in the $x - z$ plane is small for parameters near the stability line, viz. figures 2(e) and (f), and is large for parameters away from it, viz. figure 2(d).

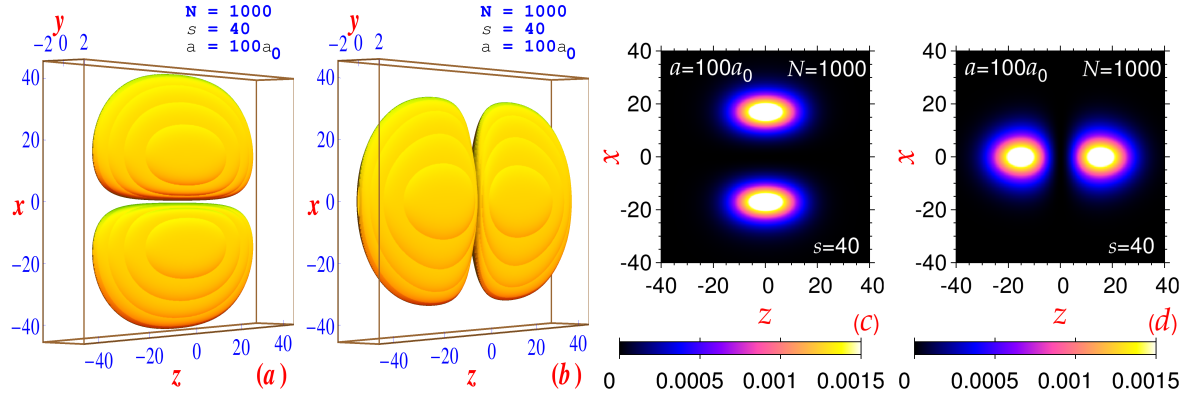


Figure 3. (Color online) 3D isodensity contour $|\phi(\mathbf{r})|^2$ of a dark-in-bright soliton of ^{164}Dy atoms in the OL trap $V(y) = s \sin^2 y/2$ with $a = 100a_0$, $N = 1000$, $s = 40$, with a notch along (a) $x = 0$ and (b) $z = 0$. The density on the contour is 0.000001. The contour plot of the 2D density $n_{2D}(x, z)$ of the two dark-in-bright solitons shown in (a) and (b), respectively, are plotted in (c) and (d).

The present dark-in-bright solitons are the stable excited states of bright dipolar solitons in the same sense as the usual dark solitons of a trapped nondipolar BEC are very unstable excitations of trapped BECs. There have been a large number of investigations about how to stabilize these nondipolar dark solitons [41, 42, 43, 44, 45, 46, 39, 40]. These studies revealed beyond any doubt that transverse snake instability of nondipolar dark solitons is an inherent property and cannot be eliminated. This casts doubt on the possibility of a decent experiment with these dark solitons. We demonstrate that the presence of dipolar interaction does not only make the dark solitons stable but also make them mobile in a plane. This opens a new scenario of performing precise experiments with the present dark-in-bright solitons. We will demonstrate how a stable dark-in-bright dipolar soliton can be realized in a laboratory by phase imprinting [35, 38] a bright soliton.

In figures 3 (a) – (b) we exhibit the 3D isodensity contour of the quasi-2D dark-in-bright solitons for $N = 1000$, $s = 40$ and $a = 100a_0$ with a notch along $x = 0$ and $z = 0$, respectively, obtained by a numerical solution of the GP equation with the OL potential starting with the initial wave function (9). The notch in the density along the x and y axes is clearly visible in figures 3 (a) and (b), respectively. For the same set of parameters (N , s and a), the dark-in-bright solitons extend over a larger domain in the $x - z$ plane compared to the bright soliton, viz. figures 2(e) and 3. In figures 3(c) and (d) we show the contour plot of the 2D density

$$n_{2D}(x, z) = \int_{-\infty}^{\infty} dy |\phi(\mathbf{r})|^2 \quad (10)$$

of the two dark-in-bright solitons of figures 3(a) and (b), respectively. These 2D contour plots show clearly the density maxima of the solitons.

We test the dynamical stability of the bright and dark-in-bright solitons of figures 2(e) and 3(a), respectively, with $N = 1000$, $a = 100a_0$, and $s = 40$ by real-time

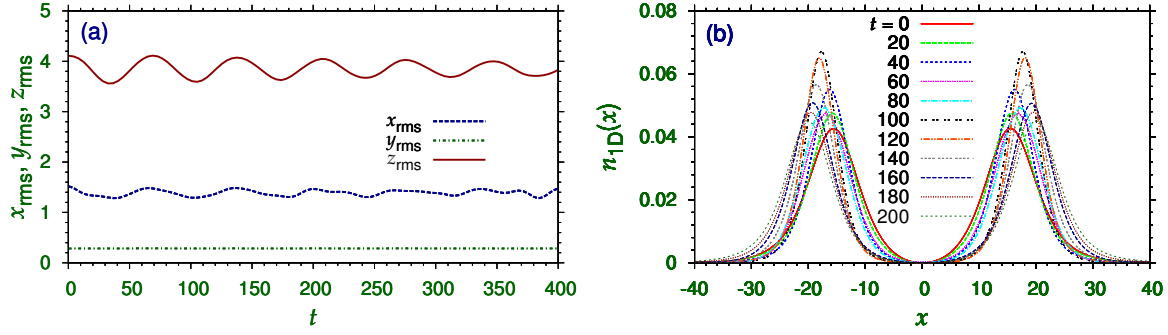


Figure 4. (Color online) Stability test of a quasi-2D (a) bright and (b) dark-in-bright soliton with $N = 1000$, $a = 100a_0$, $s = 40$. (a) Plot of rms sizes x_{rms} , y_{rms} , z_{rms} vs. time t of the bright soliton of figure 2(e) during real-time evolution of the bright soliton with the pre-calculated initial stationary state. At the start of real-time evolution at $t = 0$ the scattering length a is changed from $100a_0$ to $99a_0$. (b) Integrated 1D density $n_{1D}(x)$ vs. x of the dark-in-bright soliton of figure 3(a) at different times during real-time evolution of the dark-in-bright soliton. At $t = 0$ the scattering length a is changed from $100a_0$ to $95a_0$.

simulation with the pre-calculated stationary state. First we consider the stability of the bright soliton. During real-time evolution of the bright soliton of figure 2(e) the scattering length was changed from $a = 100a_0$ to $99a_0$ at $t = 0$. The subsequent evolution of the root-mean-square (rms) sizes x_{rms} , y_{rms} , z_{rms} is shown in figure 4(a). The sustained oscillation of the rms sizes guarantees the stability of the bright soliton. Next we consider the stability of the dark-in-bright soliton. The dark-in-bright soliton of figure 3(a) has a notch at $x = 0$. In a time evolution (real-time simulation or experiment) of a normal trapped dark soliton, the position of the notch oscillates around the center (snake instability) and eventually the dark soliton is destroyed [39, 40]. It will be interesting to see if the notch moves away from center at $x = 0$ during real-time evolution of the present dark-in-bright soliton. To test this snake instability, we plot the linear (1D) density along x direction, defined by

$$n_{1D}(x) = \int_{-\infty}^{\infty} dy \int_{-\infty}^{\infty} dz |\phi(\mathbf{r})|^2, \quad (11)$$

in figure 4(b) at different times t during real-time evolution after a change of the scattering length a from $100a_0$ to $95a_0$ at $t = 0$. Because of the large perturbation, the linear density is found to oscillate, however, maintaining the notch fixed at $x = 0$. The rms sizes also oscillate around a mean value (not shown here) as in the case of the bright soliton shown in figure 4(a). This illustrates clearly that the notch remains intact for a long time and the dark-in-bright soliton is dynamically stable.

As the quasi-2D dipolar dark-in-bright solitons are dynamically stable without any snake instability, these can be created by real-time simulation from the following phase-imprinted Gaussian profiles

$$\phi(\mathbf{r}) = \phi(\mathbf{r}), \quad x \geq 0; \quad \phi(\mathbf{r}) = -\phi(\mathbf{r}), \quad x < 0, \quad (12)$$

$$\phi(\mathbf{r}) = \phi(\mathbf{r}), \quad z \geq 0; \quad \phi(\mathbf{r}) = -\phi(\mathbf{r}), \quad z < 0, \quad (13)$$

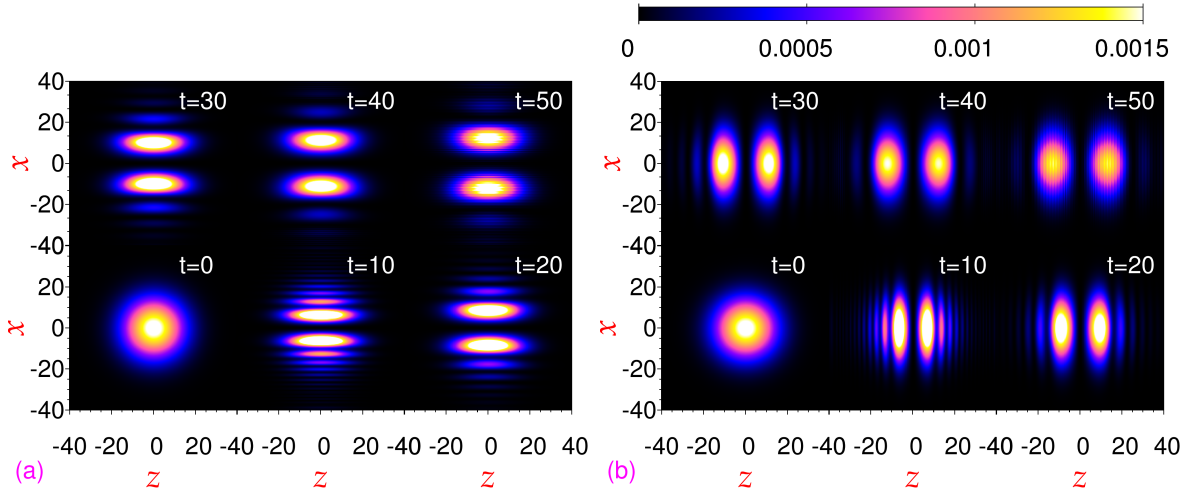


Figure 5. (Color online) Creating the quasi-2D dark-in-bright solitons of (a) figure 4(a) and (b) figure 4(b) by real-time evolution with parameters $N = 1000, a = 100a_0, s = 40$ starting from initial phase-imprinted Gaussian profiles $\phi(x, y, z) = -\phi(-x, y, z)$ and $\phi(x, y, z) = -\phi(x, y, -z)$, respectively, at $t = 0$.

respectively, for a notch along $x = 0$ and $z = 0$, where $\phi(\mathbf{r})$ is the bright soliton (8). The real-time simulation is started with this wave function. In an actual experiment a homogeneous potential generated by the dipole potential of a far detuned laser beam is applied on part of the Gaussian profile ($x < 0$ or $z < 0$) for a time interval appropriate to imprint an extra phase π on that part of the wave function. In the experiment the Gaussian profile should be the quasi-2D bright soliton with the same number of atoms N and scattering length a . In the present real-time simulation the analytic Gaussian profile (8) with $w_x = w_z = 15, w_y = 1$ is employed with the appropriate parameters: $N = 1000, a = 100a_0$ and $s = 40$. During real-time simulation the phase-imprinted Gaussian profile slowly transforms into a quasi-2D dipolar dark-in-bright soliton. Although the present real-time simulation is done with no trap, in an experiment a weak in-plane trap can be used during generating the quasi-2D dark-in-bright soliton starting from a quasi-2D bound state. The in-plane trap should be eventually removed. The result of simulation is displayed in figures 5(a) and (b) for the dark-in-bright solitons with a notch along $x = 0$ and $z = 0$, respectively, where we show the contour plot of the 2D density $n_{2D}(x, z)$ at different times. It is illustrated that at large times the density of the two dark-in-bright solitons of figures 5(a) and (b) evolves towards that of the quasi-2D dark-in-bright solitons of figures 3(c) and (d), respectively.

To demonstrate further the stability and robustness of the solitons we consider the frontal collision of two solitons of figure 2(d), with $N = 100, a = 40a_0$ and $s = 40$, moving along the x axis in opposite directions with a medium velocity. The initial number of atoms N ($= 100$) in each soliton is chosen in such a way that during collision of two solitons there is no collapse as found in a recent investigation [57]. This will require a value of $N_{crit} > 200$ in figure 1 for $a = 40a_0$. The constant velocity of about

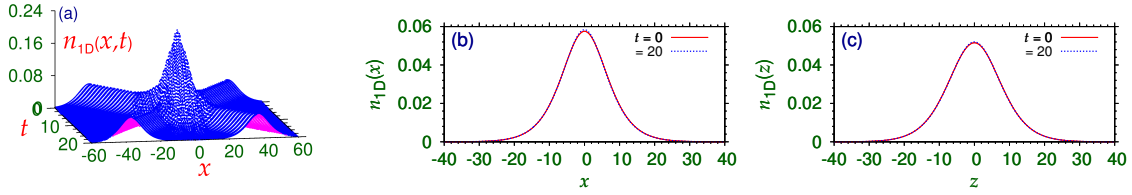


Figure 6. (Color online) (a) Frontal collision dynamics, of two identical solitons of figure 2(d) initially placed at $x = \pm 40$ and moving in opposite directions along the x axis each with speed 4, via a plot of integrated linear density $n_{1D}(x, t)$ versus x and t . (b) Initial ($t = 0$) and final ($t = 20$) integrated linear densities $n_{1D}(x)$ and $n_{1D}(z)$ of one of the two solitons undergoing frontal collision shown in (a).

4 was attributed to two solitons at $x = \pm 40$ by multiplying the soliton wave functions by factors $\exp(\pm i 20x)$. Although the solitons are capable of moving in the $x - z$ plane these phase factors will give the solitons a non-zero velocity along the x axis. The initial wave functions were pre-calculated by imaginary-time propagation. In figure 6(a) we plot the integrated 1D density $n_{1D}(x, t)$ of the dynamics of collision obtained by a real-time simulation of the GP equation. In figure 6(b) and (c) we plot the integrated initial ($t = 0$) and final ($t = 20$) 1D densities $n_{1D}(x)$ and $n_{1D}(z)$, respectively, of one of the two solitons undergoing collision. After the collision the solitons emerge quasi unchanged demonstrating the solitonic nature. For the chosen set of parameters no oscillation in the shape of emerging solitons was found as noted in Ref. [57].

4. Conclusion

We demonstrated the possibility of creating stable quasi-2D bright and dark-in-bright solitons in dipolar BEC mobile in a plane ($x - z$) containing the polarization direction (z). The quasi-2D geometry is obtained by an OL trap in the y direction. The result and finding are illustrated by a numerical solution of the time-dependent mean-field GP equation in 3D with realistic values of contact and dipolar interactions of ^{164}Dy atoms. The solitons are found to execute sustained breathing oscillation upon a small perturbation. The dark-in-bright soliton can be created in real-time simulation starting from an initial bright soliton, where an extra phase of π is introduced in the appropriate half. No dynamical instability is found in the real-time evolution of the dark-in-bright soliton after introducing a small perturbation. By real-time simulation we demonstrate the elastic nature of the frontal collision between two quasi-2D solitons. The results and conclusions of the present paper can be tested in experiments with present-day know-how and technology and should lead to interesting future investigations.

The work has been supported by the Fundação de Amparo à Pesquisa do Estado de São Paulo Project 2012/00451-0 (Brazil) and the Conselho Nacional de Desenvolvimento Científico e Tecnológico Project 303280/2014-0 (Brazil).

- [1] Abdullaev F K, Gammal A, Kamchatnov A M and Tomio L (2005) *Int. J. Mod. Phys. B* **19** 3415
- [2] Kivshar Y S and Malomed B A 1989 *Rev. Mod. Phys.* **61** 763
- [3] Perez-Garcia V M, Michinel H and Herrero H 1998 *Phys. Rev. A* **57** 3837
- [4] Strecker K E, Partridge G B, Truscott A G and Hulet R G 2002 *Nature* **417** 150
- [5] Khaykovich L, Schreck F, Ferrari G, Bourdel T, Cubizolles J, Carr L D, Castin Y and Salomon C 2002 *Science* **256** 1290
- [6] Cornish S L, Thompson S T and Wieman C E 2006 *Phys. Rev. Lett.* **96** 170401
- [7] Inouye S *et al.* 1998 *Nature* **392** 151
- [8] Griesmaier A, Werner J, Hensler S, Stuhler J and Pfau T 2005 *Phys. Rev. Lett.* **94** 160401
- [9] Lu M, Burdick N Q, Seo Ho Youn and Lev B L 2011 *Phys. Rev. Lett.* **107** 190401
- [10] Aikawa K, Frisch A, Mark M, Baier S, Rietzler A, Grimm R and Ferlaino F 2012 *Phys. Rev. Lett.* **108** 210401
- [11] Lahaye T, Koch T, Frohlich B, Fattori M, Metz J, Griesmaier A, Giovanazzi S and Pfau T 2007 *Nature* **448** 672
- [12] Griesmaier A, Stuhler J, Koch T, Fattori M, Pfau T and Giovanazzi S 2006 *Phys. Rev. Lett.* **97** 250402
- [13] Ticknor C, Wilson R M and Bohn J L 2011 *Phys. Rev. Lett.* **106** 065301
- [14] Baillie D, Bisset R N, Ticknor C and Blakie P B 2014 *Phys. Rev. Lett.* **113** 265301
- [15] Shirley W E, Anderson B M, Clark C W and Wilson R M 2014 *Phys. Rev. Lett.* **113** 165301
- [16] Armaitis J, Duine R A and Stoof H T C 2013 *Phys. Rev. Lett.* **111** 215301
- [17] Wilson R M, Anderson B M and Clark C W 2013 *Phys. Rev. Lett.* **111** 185303
- [18] Bismut G, Laburthe-Tolra B, Maréchal E, Pedri P, Gorceix O and Vernac L 2012 *Phys. Rev. Lett.* **109** 155302
- [19] Maluckov A, Gligorić G, Hadžievski L, Malomed B A and Pfau T 2012 *Phys. Rev. Lett.* **108** 140402
- [20] Wilson R M, Ronen S and Bohn J L 2010 *Phys. Rev. Lett.* **104** 094501
- [21] Young-S L E, Muruganandam P and Adhikari S K 2011 *J. Phys. B* **44** 101001
- [22] Nath R, Pedri P and Santos L 2009 *Phys. Rev. Lett.* **102** 050401
- [23] Pedri P and Santos L 2005 *Phys. Rev. Lett.* **95** 200404
- [24] Tikhonenkov I I, Malomed B A and Vardi A 2008 *Phys. Rev. Lett.* **100** 090406
- [25] Köberle P, Zajec D, Wunner G and Malomed B A 2012 *Phys. Rev. A* **85** 023630
- [26] Eichler R, Zajec D, Köberle P, Main J and Wunner G 2012 *Phys. Rev. A* **86** 053611
- [27] Zhang A-X and Xue J-K 2010 *Phys. Rev. A* **82** 013606
- [28] Adhikari S K 2016 *Laser Phys. Lett.* **13** 035502
- [29] Adhikari S K and Muruganandam P 2012 *J. Phys. B* **45** 045301
- [30] Tikhonenkov I, Malomed B A and Vardi A 2008 *Phys. Rev. A* **78** 043614
- [31] Adhikari S K 2014 *Phys. Rev. A* **90** 055601
- [32] Eiermann B, Anker Th, Albiez M, Taglieber M, Treutlein P, Marzlin K-P and Oberthaler M K 2004 *Phys. Rev. Lett.* **92** 230401
- [33] Muruganandam P and Adhikari S K 2011 *J. Phys. B* **44** 121001
- [34] Ronen S, Bortolotti D C E and Bohn J L 2007 *Phys. Rev. Lett.* **98** 030406
- [35] Burger S, Bongs K, Dettmer S, Ertmer W, Sengstock K, Sanpera A, Shlyapnikov G V and Lewenstein M 1999 *Phys. Rev. Lett.* **83** 5198
- [36] Anderson B P, Haljan P C, Regal C A, Feder D L, Collins L A, Clark C W and Cornell E A 2001 *Phys. Rev. Lett.* **86** 2926
- [37] Denschlag J *et al.* 2000 *Science* **287** 97
- [38] Dobrek L, Gajda M, Lewenstein M, Sengstock K, Birkel G and Ertmer W 1999 *Phys. Rev. A* **60** R3381
- [39] Busch Th and Anglin J R 2000 *Phys. Rev. Lett.* **84** 2298
- [40] Muryshv A, Shlyapnikov G V, Ertmer W, Sengstock K and Lewenstein M 2002 *Phys. Rev. Lett.* **89** 110401
- [41] Toikka L A and Suominen K-A 2013 *Phys. Rev. A* **87** 043601

- [42] Crosta M, Fratalocchi A and Trillo S 2011 *Phys. Rev. A* **84** 063809
- [43] Ma M, Carretero-Gonzalez R, Kevrekidis P G, Frantzeskakis D J and Malomed B A 2010 *Phys. Rev. A* **82** 023621
- [44] Efremidis N, Hizanidis K, Nistazakis H E, Frantzeskakis D J and Malomed B A 2000 *Phys. Rev. E* **62** 7410
- [45] Feder D L, Pindzola M S, Collins L A, Schneider B I and Clark C W 2000 *Phys. Rev. A* **62** 053606
- [46] Johansson M and Kivshar Y S 1999 *Phys. Rev. Lett.* **82** 85
- [47] Kishor Kumar R, Young-S L E, Vudragović D, Balaž A, Muruganandam P, Adhikari S K 2015 *Comput. Phys. Commun.* **195** 117
- [48] Muruganandam P and Adhikari S K 2009 *Comput. Phys. Commun.* **180** 1888
- [49] Goral K and Santos L 2002 *Phys. Rev. A* **66** 023613
- [50] Koch T, Lahaye T, Metz J, Fröhlich B, Griesmaier A and Pfau T 2008 *Nature Phys.* **4** 218
- [51] Muruganandam P and Adhikari S K 2003 *J. Phys. B* **36** 2501
- [52] Vudragović D, Vidanović I, Balaž A, Muruganandam P and Adhikari S K 2012 *Comput. Phys. Commun.* **183** 2021
- [53] Satarić B, Slavnić V, Belić A, Balaž A, Muruganandam P and Adhikari S K 2016 *Comput. Phys. Commun.* **200** 411
- [54] Loncar V, Balaž A, Bogojević A, Skrbić S, Muruganandam P and Adhikari S K 2016 *Comput. Phys. Commun.* **200** 406
- [55] Gammal A, Frederico T and Tomio L 2001 *Phys. Rev. A* **64** 055602
- [56] Adhikari S K 2001 *Phys. Rev. E* **65** 016703
- [57] Nguyen J H V, Dyke P, Luo D, Malomed B A and Hulet R G 2014 *Nature Phys.* **10** 918